Desalination and Water Treatment
www.deswater.com
doi: 10.5004/dwt.2020.25079

180 (2020) 37–42
March

Performance and antifouling behaviour of nanoclay incorporated polysulfone ultrafiltration membrane for wastewater treatment

Jacob Lovey*, Joseph Shiny*, Varghese Lity Alen

Department of Chemical Engineering, NIT Calicut, Kerala-673601, India, emails: loveyjacob@gmail.com (J. Lovey), shiny@nitc.ac.in (J. Shiny), lityalen@nitc.ac.in (V.L. Alen)

Received 30 April 2019; Accepted 22 October 2019

ABSTRACT

Montmorillonite clay (MMT) modified with dimethyl dialkyl amine (mMMT) are introduced to transform the hydrophobic polysulfone (psf) ultrafiltration membranes into hydrophilic membranes. In the present work, ultrafiltration membranes are prepared using the solvent N-methyl pyrrolidone (NMP) and polyvinylpyrrolidone (PVP) as porogen by phase inversion technique and the amount of mMMT is varied from 1 to 5 wt.%. The prepared membranes are characterized by scanning electron microscopy and X-ray diffractometer. Water uptake, contact angle, and porosity of the membranes are evaluated to analyze the hydrophilicity of the membrane. Performance studies are conducted in a cross-flow filtration unit using a synthetic solution containing 5 ppm chromium(VI) ions and membranes with varying percentages of mMMT. A chromium ion rejection of 93% and a flux rate of 200 L/m^{2}h were obtained for membrane incorporated with 3% mMMT compared to a rejection of 64% and flux rate of 44 L/m^{2}h for neat psf membrane. The antifouling behavior was studied using organic foulant, bovine serum albumin (BSA) solution (100 mg/L). Antifouling studies show that for 3 wt.% mMMT, flux recovery ratio increases from 58% to 77% with the reduction of irreversible resistance from 41% to 22% and the total resistance 67% to 45% as compared to neat psf membranes. The addition of mMMT improved the chromium ion removal efficiency and antifouling property of the membrane.

Keywords: Ultrafiltration; Polysulfone; Nanoclay; Chromium removal; Antifouling

1. Introduction

Increasing the emission of heavy metals from various industries became a great threat to human beings as well as the ecosystem. Wastewater containing one of the most carcinogenic heavy metal chromium (Cr) ions are thrown out to the environment by various industries such as leather industries, electroplating industries, etc. [1]. Out of all industrial effluents, tannery effluents from leather industries contain more chromium ions, since 90% of leather industries utilize (Cr) ions as tanning substances [2]. To meet the demand for quality water, membrane technology plays a vital role in wastewater treatment due to ease of operation, compactness and high separation efficiency [3]. Polysulfone (psf) is a widely used polymer for the preparation of membranes due to its high thermal, chemical and mechanical properties. Due to the hydrophobic nature of this polymer, these membranes are easily susceptible to fouling which restricts its wide applications [4]. For enhancing the hydrophilic nature of the membrane, nanoparticles such as zeolite, nanoclay, titania, silica, etc are introduced which in turn increases the antifouling properties of the membranes [5]. Presently montmorillonite clays as an inorganic filler have gained more attention in the preparation of ultrafiltration membranes for wastewater treatment. According to the previous researches, ultrafiltration can be used as an efficient method

* Corresponding authors.

for the removal of Cr ions. From the various studies it was found that to improve the efficiency of these nanocomposite ultrafiltration membranes, nanoclay modified with quaternary ammonium groups or tertiary amine groups were introduced into the polymer matrix [1,6].

In the present study montmorillonite clay modified with dimethyl dialkyl amine (mMMT) is used as nanoparticle for evaluating the performance and antifouling properties of nanocomposite membrane. Different quantities of mMMT are introduced to investigate its effect on hydrophilicity, porosity, water uptake, and mechanical property.

2. Materials and methods

Polysulfone pellets and mMMT were purchased from Sigma-Aldrich (USA); N-methyl pyrrolidone, polyvinylpyrrolidone; were purchased from Otto chemicals, India. Distilled water was used for the preparation of ultrafiltration membranes.

2.1. Fabrication of ultrafiltration membranes

Ultrafiltration membranes are prepared using polysulfone pellets and the solvent N-methyl pyrrolidone (NMP) with the pore-forming agent polyvinylpyrrolidone (PVP) using the phase inversion technique is a well-known technique for the preparation of asymmetric membranes. Adequate amount of psf (20 wt.%), NMP (80 wt.%) and PVP (0.6 wt.%) are kept in the hot plate magnetic stirrer at 250 rpm at a temperature of 60°C. mMMT entrapped polysulfone ultrafiltration membranes are prepared by incorporating different amounts of mMMT from 1 to 5 wt.% in the psf/NMP/PVP solution. Additives are sonicated in probe sonicator for 5 min before introducing into the psf/NMP/PVP solution to ensure uniform dispersion of nanoparticles in the casting solution. Polymer film with a thickness of 200 μm is then cast on a glass plate using automatic thin-film applicator. Glass plate along with the polymer film is then dipped into the distilled water (DI) was solvent–nonsolvent interaction occurs leading to the formation of ultrafiltration membranes. The membranes thus fabricated are kept in the DI water for further analysis.

2.2. Ultrafiltration characterization

2.2.1. Water uptake

The percentage of water uptake represents the number of water molecules that occupy the pores of the membrane. Water uptake is measured by taking the weight of 24 h soaked membrane pieces in water and these membrane pieces are kept for drying in an oven for 24 h at 50°C–60°C. The dried membranes are then weighed to get the dry weight of the sample. Percentage of water uptake is calculated using the equation [7]:

$$\%\ \text{Water uptake} = \frac{\text{Wet Weight of the sanple} - \text{dry weight of the sample}}{\text{wet weight of the sample}} \times 100 \quad (1)$$

2.2.2. Porosity

Porosity represents the fraction of voids formed on the membranes during immersion precipitation. % porosity is calculated using the equation,

$$p = \frac{\left(W_1 - W_0\right)}{\left(\rho A h\right)} \times 100 \quad (2)$$

where p is the porosity of the membrane, ρ is the water density 998 kg/m^3, A is the membrane surface area (m^2), h is the membrane thickness (m), W_1 and W_0 is the wet weight and dry weight of the sample (kg) [8].

The mean pore radius of the membranes is calculated using Guerout–Elford–Ferry equation.

$$r_m = \sqrt{\frac{\left(2.9 - 1.75\varepsilon\right) \times 8\eta l\ Q}{\varepsilon A \Delta P}} \quad (3)$$

where r_m is the mean pore radius, ε is the porosity of the membrane, η is the water velocity (8.9×10^{-4} Pa s), l is the membrane thickness (m), Q is the pure water flux (m^3/s), A is the membrane area (m^2) and ΔP is the operating pressure (bar).

2.2.3. Contact angle

Surface wetting properties of the membrane play a significant role in the properties of the membrane such as pure water flux, % rejection and antifouling properties. This wettability or hydrophilicity can be determined by measuring the contact angle of a pure water drop on the surface of the membrane sample. Lower contact angle measurement indicates the hydrophilic nature of the membrane and higher value signifies the hydrophobic nature of the material [9]. Here we are using a digidrop goniometer to measure the contact angle. A microsyringe with the needle is used to provide a pure water droplet over the surface of the membrane and the contact angles were noted. Five contact angle measurements were taken from different locations of each sample and were averaged to report the same.

2.3. Permeation and analytical experiments

Permeation test is carried out using Sterlitech cross-flow filtration (USA) unit having an effective area of 42 cm^2. Fabricated membranes are compacted at a higher pressure of 7 bar to make the membrane pore size and structure rigid. Pure water flux is determined by varying the pressure from 1 to 5 bar and the solute concentration is determined using PerkinElmer UV visible spectrometer (lambda 650, USA). The concentration of 5 ppm Cr(VI) feed is fed to the cross-flow filtration unit and the experiment is carried out at an operating pressure of 2 bar. Permeate is collected at regular time intervals and the volume is noted. The flux rate and solute rejection was calculated using the equations,

$$J_0 = \frac{\Delta V}{A} \times \Delta t \quad (4)$$

where J_0 is the water flux in L/m²h, A is the effective area of membrane in m², ΔV is the volume of permeate solution in m³, Δt is the time in h.

$$R_0(\%) = \left(\frac{1-C_p}{C_f}\right)\times 100 \quad (5)$$

where C_p is the concentration of permeate solution and C_f is the concentration of feed solution.

2.4. Fouling experiments

To investigate the antifouling properties of the membranes, bovine serum albumin (BSA) is used as a model foulant. Initially, the experiment is conducted with pure distilled water and permeate is collected for a time interval until the volume became steady. The pure water flux is calculated and noted as J_0. The distilled water in the feed container is replaced with the BSA solution (100 mg/L). For a specific time interval, the volume of permeate is noted until the volume became steady and the flux rate is calculated and noted as J_1. Once the permeation of the fouled membrane becomes steady, the membrane is taken out and water flushing which is a physical cleaning method is carried out to determine flux recovery ratio (FRR), irreversible resistance (R_{ir}) reversible resistance (R_r) and total resistance (R_t) [10]. Correspondingly, feed in the feed tank is replaced by distilled water to measure pure water flux and denoted as J_2.

$$\text{FRR }\% = \left(\frac{J_2}{J_0}\right)\times 100 \quad (6)$$

$$R_r\% = \left[\frac{(J_2 - J_1)}{J_0}\right]\times 100 \quad (7)$$

$$R_{ir}\% = \left[\frac{(J_0 - J_2)}{J_0}\right]\times 100 \quad (8)$$

$$R_t\% = \left[\frac{(J_0 - J_1)}{J_0}\right]\times 100 \quad (9)$$

where J_0 is the initial flux rate.

2.5. Membrane characterisation

The membrane structure is examined by scanning electron microscopy (SEM). The cross-sectional micrographs can be used to compare the morphological changes of modified and unmodified membranes. The physical characterization is carried out using Shimadzu (USA) Autograph universal testing machine according to ASTM standards and X-ray diffraction (XRD) analysis reveals the exfoliated and intercalated structure of the nanoparticle and it accurately quantifies the *d*-spacing value of the silicate layers [11].

3. Results and discussions

3.1. Performance analysis

3.1.1. Hydrophilicity of the membranes

Surface hydrophilicity of the membrane plays a significant role in the flux rate and the antifouling properties of the membranes. The contact angle denotes the hydrophilic/hydrophobic nature of the membrane. From the Fig. 1, it is seen that the contact angle decreases from 79° to 49° then starts increasing. The decrease in the degree of the contact angle is, in turn, represents the increase in the hydrophilic nature of the membrane. This increase in the hydrophilicity may be due to the incorporation of organically modified nanoclay, which contains hydrophilic polar ammonium fractions [10]. Also, it is seen that as the concentration of nanoparticle increases up to 3 wt.% water uptake shoots up from 68% to 80% along with an increase in porosity from 54% to 77% which also indicates an increase in the hydrophilic nature of the membrane. This increase in porosity and water uptake may due to the migration of hydrophilic nanoparticle to the surface of the membrane resulted in more nanoplates [12]. Above 3 wt.% nanoparticles may get agglomerated which in turn reduces the effective surface area of the membrane resulted in lower water uptake, porosity, and higher contact angle.

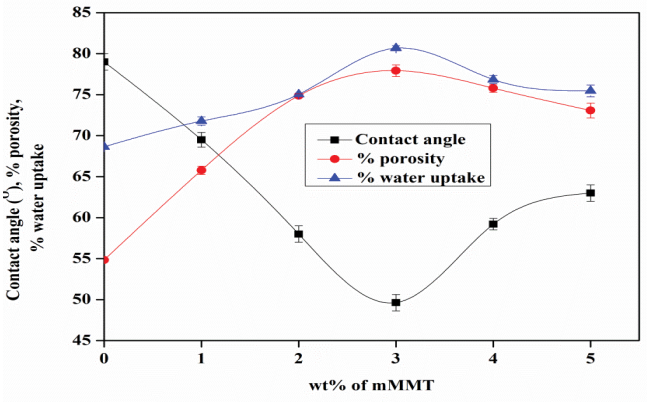

Fig. 1. Effect of mMMT on the hydrophilicity of the membranes.

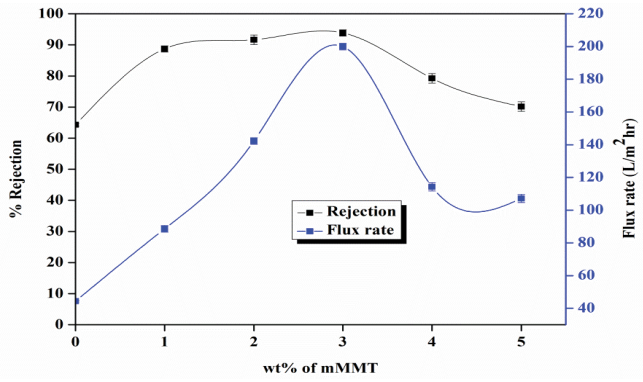

Fig. 2. Flux rate and % rejection for varying mMMT concentration.

3.1.2. Performance evaluation of the membranes

Fig. 2 shows that the concentration of mMMT increases to 3 wt.%, as the flux rate increases to 200 from 44 L/m²h and the % rejection increases from 64% to 93%. This increase in the flux rate is due to the presence of polar moieties in the mMMT as well as its layered structure. Even though the mMMT does not have a porous structure, its interlayer gallery will provide extra void space which may increase the flux rate of the membrane. An increase in the rejection of hexavalent chromium is due to the cationic-cationic repulsion as the nanoclay is modified with a quaternary ammonium group. As the concentration of mMMT increases beyond 3 wt.%, the flux rate, as well as % rejection, decreases. This is because the concentration of mMMT increases, the viscosity of the solution increases and the mMMT may act as a physical barrier that retards the solvent-nonsolvent diffusion rate during phase inversion thereby offsets the hydrophilicity of the membrane [13].

3.1.3. Mean pore radii

Table 1 shows the mean pore radii of membranes calculated using Guerout–Elford–Ferry equation for varying mMMT concentration. It is noted that pore radii have a direct relation with mMMT concentration and flux decline. From Table 1 it is seen that psf membranes without additives have lower mean pore radii resulted in the lower flux rate of 44 L/m²h. Addition of PVP and mMMT increases the pore radii of the membranes. It is also observed that as the concentration of mMMT increases until 3 wt.% mean pore radii increases, in turn, increases the flux rate of the membrane. Beyond 3 wt.%, mean pore radii decreases which may be due to the agglomeration of mMMT. This may block the pores of the membrane resulting in flux decline and Cr(VI) ion rejection.

3.2. Antifouling property evaluation of the membranes

Antifouling properties of psf membrane and 3 wt.% mMMT incorporated psf membrane were evaluated. Fig. 3 shows that by the addition of mMMT FRR shoot up from 58% to 77% along with the reduction of irreversible resistance (R_{ir}) from 41% to 22% and the total resistance (R_t) 67% to 45%. This increase in the antifouling property of the membrane by the addition of mMMT is due to the increase in the hydrophilicity of the membrane which resulted in the lower adhesion of foulant which is hydrophobic [14,15].

Table 1
Mean pore radii for varying mMMT concentration

wt.% of mMMT	Mean pore radii	Flux rate L/m²h	% Rejection
0	10.94	44.38	64.3
1	20.66	88.57	88.71
2	21.28	142.28	91.66
3	22.10	200	93.85
4	18.45	114.28	79.24
5	17.75	107.14	70.17

3.3. Characterisation studies

3.3.1. Tensile strength of the membranes

Tensile strength and % elongation of different nanocomposite membranes were measured for evaluating the mechanical behavior of the membranes. Fig. 4 shows that tensile strength and the % elongation is found to be higher for the nanocomposite membranes containing 3 wt.% mMMT. As the concentration of mMMT increases, mechanical properties increase until 3 wt.% and then start decreasing. The increase in mechanical properties is due to the uniform distribution of the mMMT which resulted in the uniform stress transfer along polymer chains and mMMT of the membrane. Further increase in the concentration of mMMT resulted in the agglomeration of mMMT as well as the non-uniform distribution of mMMT in the membrane thereby decreasing membrane tensile strength and elongation.

3.3.2. Scanning electron microscopy

Fig. 5 shows the crossectional morphologies of the polysulfone membrane and the polysulfone nanocomposite membrane containing 3 wt.% mMMT. Both membranes

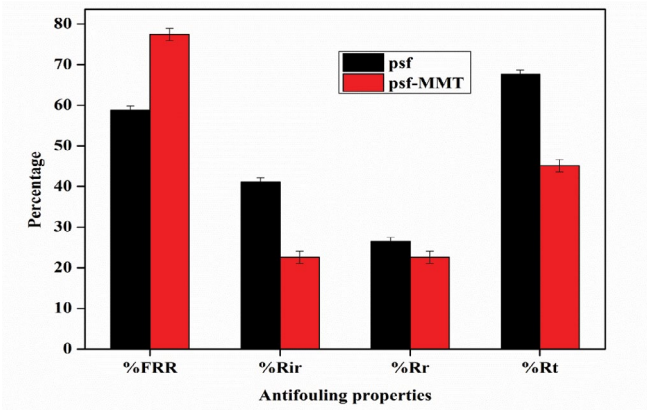

Fig. 3. Antifouling properties of psf and psf-mMMT membranes.

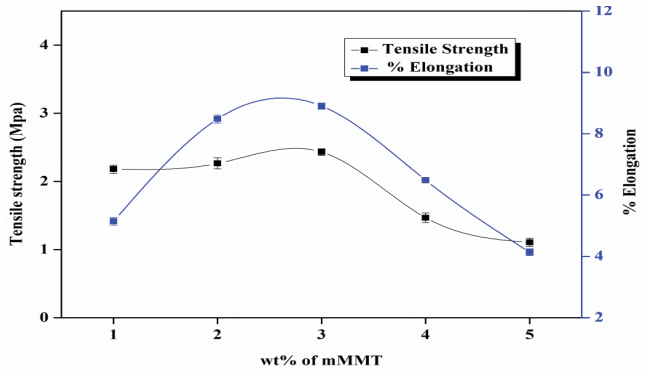

Fig. 4. Mechanical properties of membranes with varying mMMT concentration.

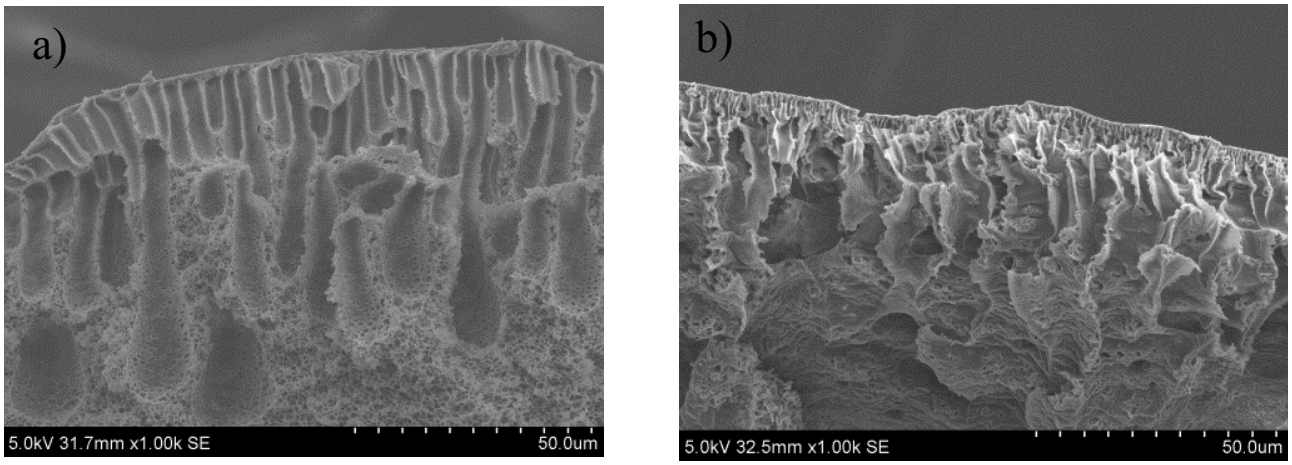

Fig. 5. SEM micrographs of (a) psf membrane and (b) psf-mMMT membrane.

exhibit a unique asymmetric structure having a denser top layer and a porous sublayer. SEM image of the nanocomposite membrane showed that by the addition of mMMT, the bottom surface layer of the membrane is having more cavities with a more finger-like pore structure which is due to the instantaneous demixing of casting solution by the addition of highly hydrophilic mMMT.

3.3.3. X-ray diffraction

Morphological studies of ultrafiltration membranes are conducted by utilizing the XRD analysis. XRD pattern of prepared psf membrane and polymer nanocomposite membranes contains 3 wt.% mMMT are depicted in Fig. 6. *d*-spacing value of nanocomposite membrane and neat membrane is found to be 5.2 and 4.9. This shows that by the addition of mMMT, *d*-spacing value increases which in turn indicates the penetration of polymer chains into the silicate layer. This confirms the intercalated nanocomposite formation which resulted in the higher hydrophilicity of the membrane.

4. Conclusion

Ultrafiltration membranes of neat polysulfone and nanocomposite membranes are successfully prepared for the removal of Cr(VI) by phase inversion techniques. It is found that as the concentration of mMMT increases, %water uptake and %porosity of the membrane increases up to 3 wt.% and the decrease in the contact angle from 79° to 49° for 3 wt.% mMMT shows that the addition of mMMT improves the hydrophilicity of the membranes. %Rejection and flux rate are found to be higher for 3 wt.% mMMT psf membranes. It was found that % rejection increases from 64% to 93% and the flux rate increases from 44 to 200 L/m^{2}h. By evaluating the mechanical properties of the nanocomposite membranes it was found that the tensile strength increases as compared to neat psf membranes along with % elongation. Based on the results of the present experiments it was found that membranes with 3 wt.% mMMT are having better hydrophilicity, flux rate and % rejection along with better antifouling characteristics. XRD results show that d-spacing value increases for 3 wt.% mMMT incorporated membrane to 5.2 from 4.9 nm as that of neat psf membrane. From the SEM images, it was observed that the more finger-like macrovoids structure is formed in the membrane sublayer by the addition of mMMT. Owing to higher antifouling property, FRR, mechanical strength and % rejection, the polysulfone/mMMT, composite membranes can be used as antifouling membranes for removal of heavy metals from wastewater.

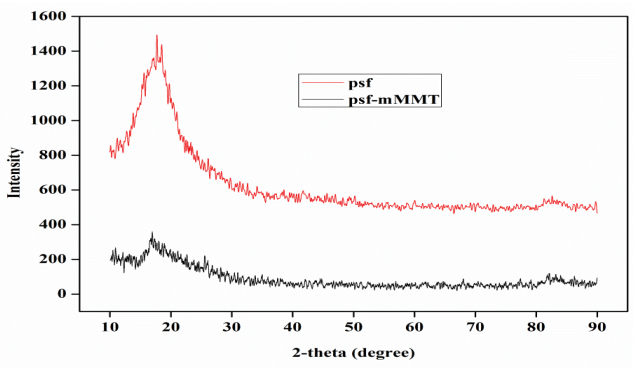

Fig. 6. XRD images of psf membrane and mMMT membrane.

Acknowledgment

This research did not receive any specific funding.

References

[1] Z. Yao, S. Du, Y. Zhang, B. Zhu, L. Zhu, A.E. John, Positively charged membrane for removing low concentration Cr(VI) in ultrafiltration process, J. Water Process Eng., 8 (2015) 99–107.
[2] A.A. Belay, Impacts of chromium from tannery effluent and evaluation of alternative treatment options, J. Environ. Prot., 1 (2010) 53–58.
[3] A. Khan, T.A. Sherazi, Y. Khan, S. Li, S. Ali, R. Naqvi, Fabrication and characterization of polysulfone/modified nanocarbon black composite antifouling ultrafiltration membranes, J. Membr. Sci., 554 (2018) 71–82.
[4] S. Xiao, S. Yu, L. Yan, Y. Liu, X. Tan, Preparation and properties of PPSU/GO mixed matrix membrane, Chin. J. Chem. Eng., 25 (2017) 408–414.

[5] J. Lin, W. Ye, K. Zhong, J. Shen, N. Jullok, A. Sotto, B. Van der Bruggen, Enhancement of polyethersulfone (PES) membrane doped by monodisperse Stöber silica for water treatment, Chem. Eng. Process., 107 (2016) 194–205.
[6] T. Felbeck, A. Bonk, G. Kaup, S. Mundinger, T. Grethe, M. Rabe, U. Vogt, U. Kynast, Porous nanoclay polysulfone composites: a backbone with high pore accessibility for functional modifications, Microporous Mesoporous Mater., 234 (2016) 107–112.
[7] P.A. Vinodhini, P.N. Sudha, Removal of heavy metal chromium from tannery effluent using ultrafiltration membrane, Text. Clothing Sustainable, 2 (2017) 5.
[8] G. Arthanareeswaran, D. Mohan, M. Raajenthiren, Preparation, characterization and performance studies of ultrafiltration membranes with polymeric additive, J. Membr. Sci., 350 (2010) 130–138.
[9] R.S. Hebbar, A.M. Isloor, A.F. Ismail, Contact Angle Measurements, Membr. Charact., Elsevier, B.V, 2017, pp. 219–255.
[10] H. Rajabi, N. Ghaemi, S.S. Madaeni, P. Daraei, M.A. Khadivi, M. Falsafi, Nanoclay embedded mixed matrix PVDF nanocomposite membrane: preparation, characterization and biofouling resistance, Appl. Surf. Sci., 313 (2014) 207–214.
[11] P. Daraei, S. Madaeni, E. Salehi, N. Ghaemi, H. Sadeghi Ghari, M.A. Khadivi, E. Rostami, Novel thin film composite membrane fabricated by mixed matrix nanoclay/chitosan on PVDF microfiltration support: preparation, characterization and performance in dye removal, J. Membr. Sci., 436 (2013) 97–108.
[12] M. Mahmoudian, P.G. Balkanloo, Clay-hyperbranched epoxy/polyphenylsulfone nanocomposite membranes, Iran. Polym. J., 26 (2017) 711–720.
[13] P.S. Goh, B.C. Ng, W.J. Lau, A.F. Ismail, Inorganic nanomaterials in polymeric ultrafiltration membranes for water treatment, Sep. Purif. Rev., 44 (2015) 216–249.
[14] V. Vatanpour, S.S. Madaeni, R. Moradian, S. Zinadini, B. Astinchap, Fabrication and characterization of novel antifouling nanofiltration membrane prepared from oxidized multiwalled carbon nanotube/polyethersulfone nanocomposite, J. Membr. Sci., 375 (2011) 284–294.
[15] H. Dong, L. Wu, L. Zhang, C. Gao, Clay nanosheets as charged filler materials for high-performance and fouling-resistant thin film nanocomposite membranes, J. Membr. Sci., 494 (2015) 92–103.